

Supporting information (SI) for

Remarkable changes in the photoluminescent properties of $\text{Y}_2\text{Ce}_2\text{O}_7:\text{Eu}^{3+}$ red phosphors through the modification of cerium oxidation states and oxygen vacancy ordering

Athira K.V. Raj, P. Prabhakar Rao*, T. S. Sreena, S. Sameera, Vineetha James and U. A. Renju

Materials Science and Technology Division, CSIR-National Institute for Interdisciplinary Science and Technology (NIIST), Trivandrum – 695 019, India

ESI. Calculation Procedure for Judd–Ofelt intensity parameters

The Judd–Ofelt intensity parameters of the $\text{Y}_2\text{Ce}_{2-x}\text{O}_7:x\text{Eu}^{3+}$ ($x = 0, 0.05, 0.20, 0.25,$ and 0.50) are summarized in Table 3 of the manuscript and is calculated from the luminescence emission spectrum. The integrated emission intensities (areas below the luminescence bands) are associated with the radiative emission rates and can be written as:

$$\frac{A_{0-2,4}}{A_{0-1}} = \frac{I_{0-2,4} h\nu_{0-1}}{I_{0-1} h\nu_{0-2,4}}$$

(1)

where I_{0-J} is the integrated emission intensity and $h\nu_{0-J}$ is the energy corresponding to transition ${}^5\text{D}_0 \rightarrow {}^7\text{F}_J$ ($J = 1, 2, 4$). The transition ${}^5\text{D}_0 \rightarrow {}^7\text{F}_1$ is left out due to their small emission intensities. The magnetic dipole radiative emission rate A_{0-1} has a value of $\approx 50 \text{ s}^{-1}$. The radiative emission rates $A_{0-2,4}$ are related to forced electric dipole transitions and they may be written as a function of the J–O intensity parameters:

$$A_{0-J} = \frac{64\pi^4(\nu_{0-2,4})^3 e^2}{3hc^3} \frac{1}{4\pi\epsilon_0} \chi \sum_{j=2,4,6} \Omega_j \langle 5D_0 | U^{(j)} | 7F_{2,4} \rangle^2 \quad (2)$$

where, χ is the Lorentz local field correction factor given as function of the index of refraction n of the host $\chi = n(n^2 + 2)^{2/3}$. The non-zero square reduced matrix elements are solely $\langle 5D_0 | U^{(2)} | 7F_2 \rangle^2 = 0.0032$ and $\langle 5D_0 | U^{(4)} | 7F_4 \rangle^2 = 0.0023$. Thus, using Eqs. (1) and (2) the values of $\Omega_{2,4}$ were obtained. The value of Ω_6 could also be estimated by analysing the ${}^5D_0 \rightarrow {}^7F_6$ transition but in the present case, this emission could not be observed. The calculated Judd–Ofelt parameters have been used to predict some important radiative properties such as transition probabilities, radiative lifetime and branching ratios and lifetimes for the excited states of Eu^{3+} ions. The radiative transition probability for a transition $\Psi J \rightarrow \Psi' J'$ can be calculated from Eq. (3) as $A_{rad}(\Psi J, \Psi' J') = A_{J-J'}$.

The total radiative transition probability (A_T) can be calculated using the equation below:

$$A_T(\Psi J) = \sum_{J'} A_{J-J'} \quad (3)$$

The radiative lifetime $\tau_{rad}(\Psi J)$ of an excited state in terms of A_T , is given by:

$$\tau_{rad}(\Psi J) = \frac{1}{A_T(\Psi J)}$$

(4)

The branching ratio $\beta(\Psi J)$ corresponding to the emission from an excited level to its lower levels is given by:

$$\beta(\Psi J) = \frac{A(\Psi J, \Psi' J')}{A_T(\Psi J)}$$

(5)

The stimulated emission cross-section ($\sigma(\lambda_p)$) can be expressed as:

$$(\sigma(\lambda_p))(J \rightarrow J') = \frac{\lambda_p^4}{8\pi c n^2 \Delta\lambda_{eff}} A_{rad}(J \rightarrow J') \quad (6)$$

where λ_p is the peak wavelength and $\Delta\lambda_{eff}$ is its effective line width found by dividing the area of the emission band by its maximum height.

ESI. Calculation Procedure for Quantum Efficiency

Assuming that only radiative and non radiative processes are essentially involved in the depopulation of 5D_0 states of Eu^{3+} ion, the quantum efficiency (η) can be expressed as;

$$\eta = A_{rad}/(A_{rad} + A_{nrad}) \quad (7)$$

where A_{rad} and A_{nrad} are radiative and non radiative transition probabilities respectively

Figure Captions

Fig. S1. Powder XRD patterns of $Y_2Ce_{1-x}O_7:xEu^{3+}$ ($x = 0.05, 0.10, 0.15, 0.20, 0.25, 0.50$) red phosphors. The XRD patterns can be indexed completely to the C-type structure.

Fig. S2. XPS spectra of Ce 3d for $Y_2Ce_{1.5}O_7:0.5Eu^{3+}$ red phosphor and the concentration of Ce^{3+} state is decreased compared to the lower substituted one ($x = 0.10$) and is found to be 11.5%.

Fig. S3. Selected area electron diffraction patterns (SEAD) and TEM micrographs (a) $Y_2Ce_{1.8}O_7:0.2Eu^{3+}$ and (b) $Y_2Ce_{1.5}O_7:0.5Eu^{3+}$ red phosphors.

Fig. S4. Energy dispersive spectrometer (EDS) spectra of (a) $\text{Y}_2\text{Ce}_{1.8}\text{O}_7:0.2\text{Eu}^{3+}$ and (b) $\text{Y}_2\text{Ce}_{1.5}\text{O}_7:0.5\text{Eu}^{3+}$ red phosphors.

Fig. S5. Typical SEM images of $\text{Y}_2\text{Ce}_{2-x}\text{O}_7:x\text{Eu}^{3+}$ ($x = 0.05, 0.10, 0.15, 0.20, 0.25$ and 0.50) red phosphors. The particles are slightly agglomerated and there is a broad distribution of particle size with an average size of 1-3 μm .

Fig. S1.

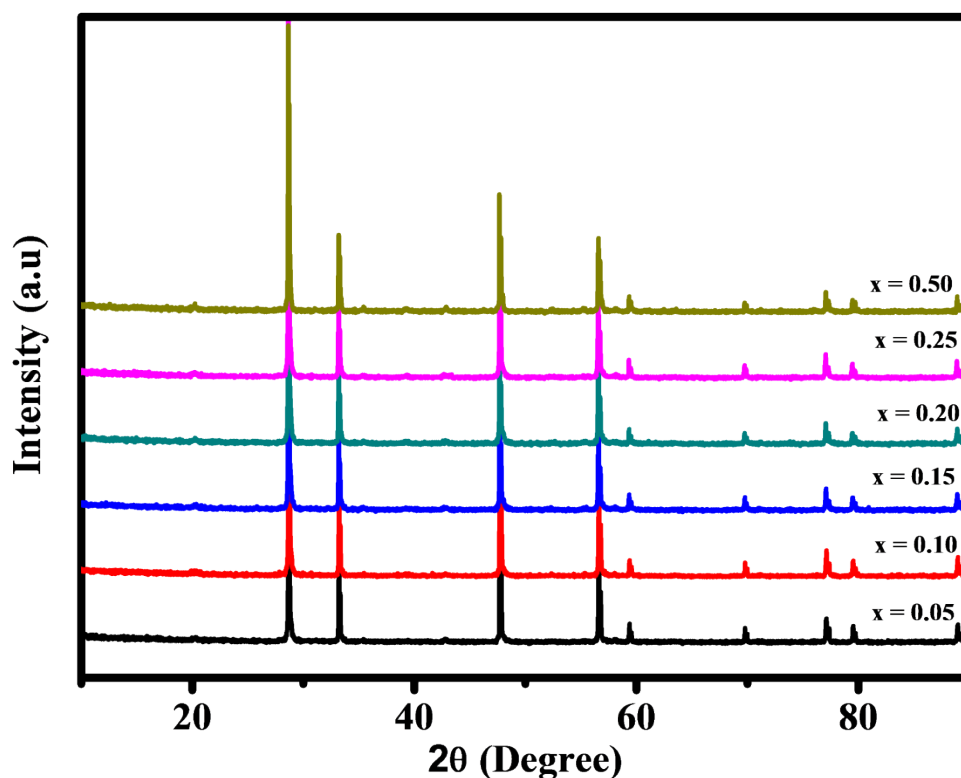


Fig. S1. Powder XRD patterns of $\text{Y}_2\text{Ce}_{1-x}\text{O}_7:x\text{Eu}^{3+}$ ($x = 0.05, 0.10, 0.15, 0.20, 0.25, 0.50$) red phosphors. The XRD patterns can be indexed completely to the C-type structure.

Fig. S2.

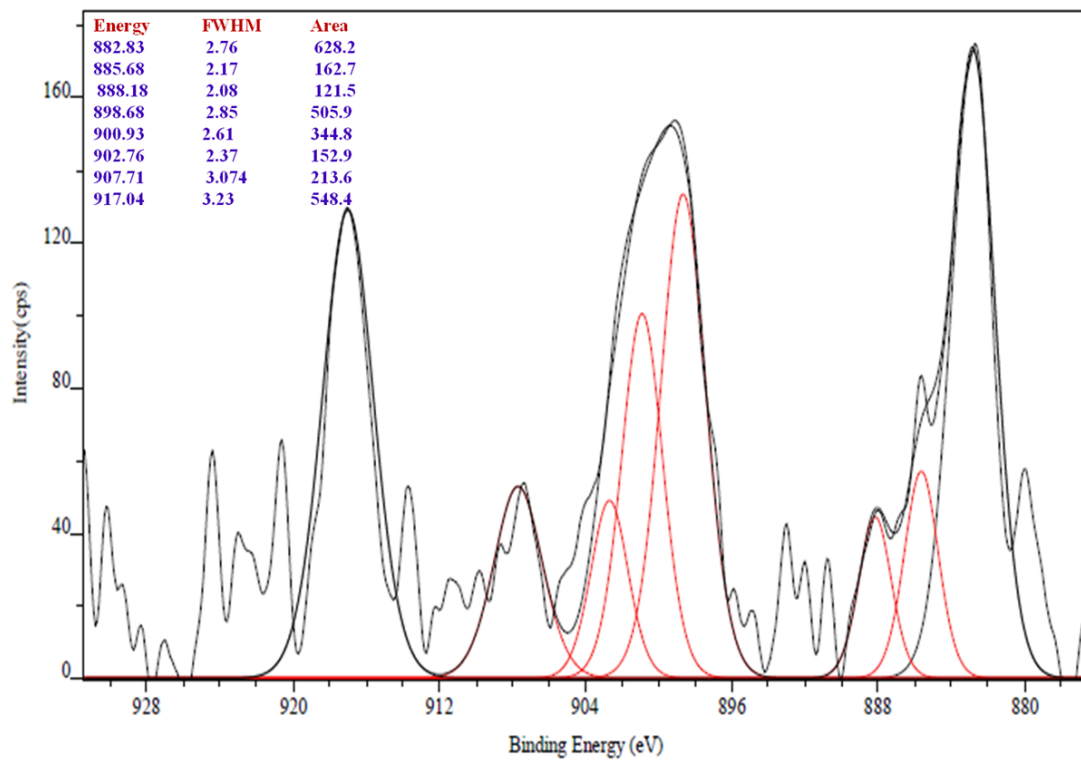


Fig. S2. XPS spectra of Ce 3d for Y₂Ce_{1.5}O₇:0.5Eu³⁺ red phosphor and the concentration of Ce³⁺ state is decreased compared to the lower substituted one ($x = 0.10$) and is found to be 11.5%.

Fig. S3.

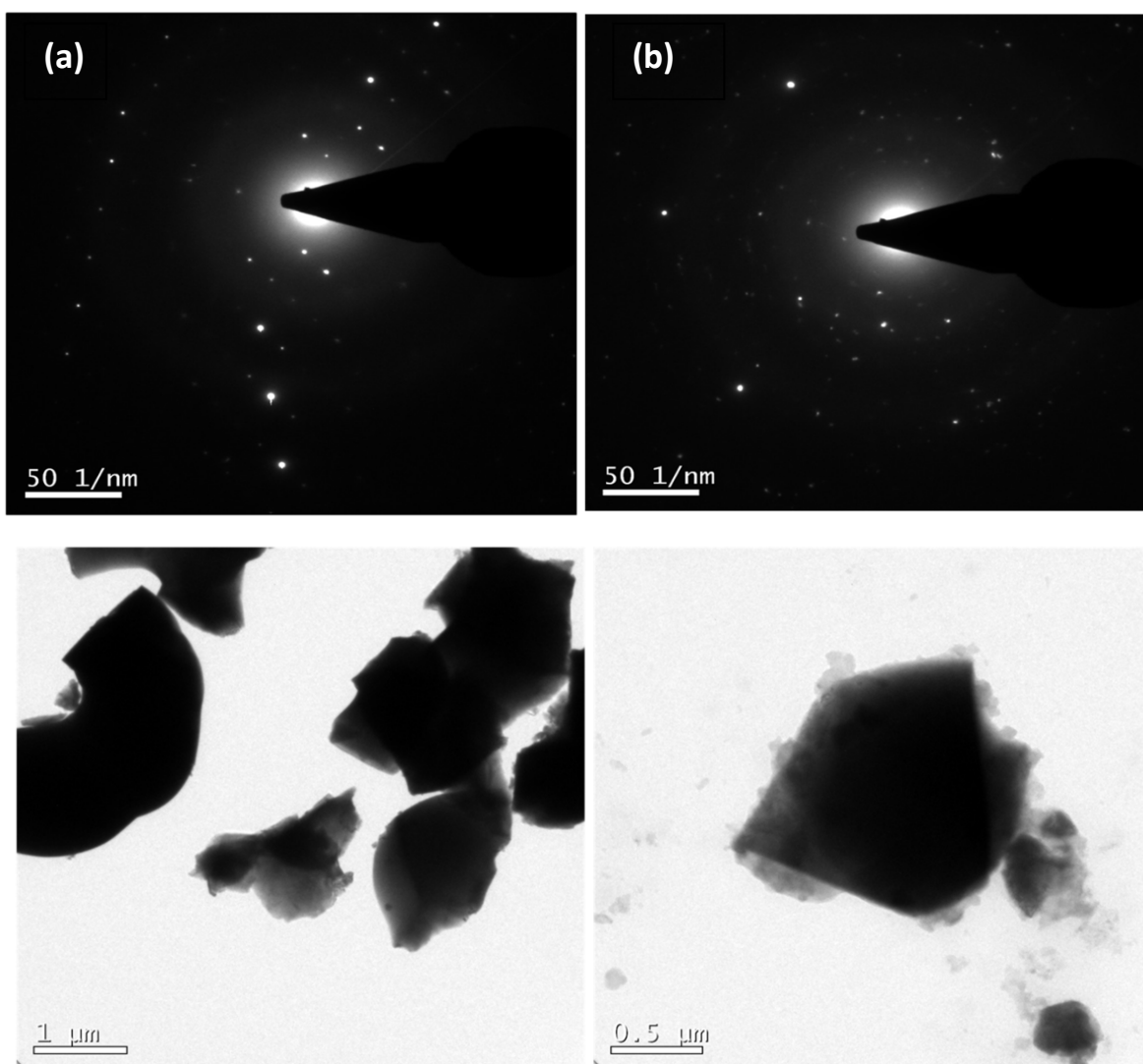


Fig. S3. Selected area electron diffraction patterns (SEAD) and TEM micrographs (a) $Y_2Ce_{1.8}O_7:0.2Eu^{3+}$ and (b) $Y_2Ce_{1.5}O_7:0.5Eu^{3+}$ red phosphors.

Fig. S4.

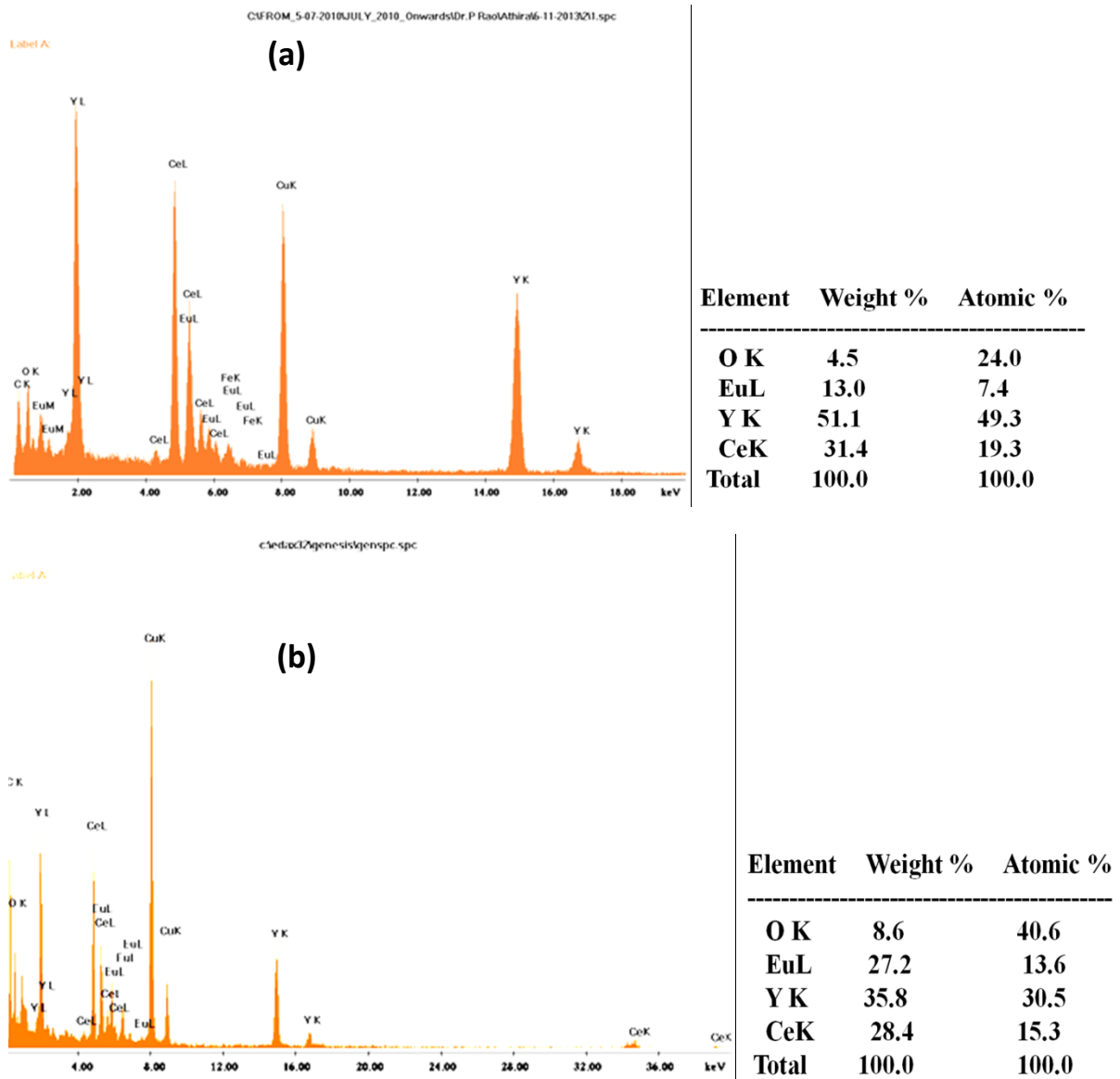


Fig. S4. Energy dispersive spectrophotometer (EDS) spectra of (a) $\text{Y}_2\text{Ce}_{1.8}\text{O}_7:0.2\text{Eu}^{3+}$ and (b) $\text{Y}_2\text{Ce}_{1.5}\text{O}_7:0.5\text{Eu}^{3+}$ red phosphors.

Fig. S5.

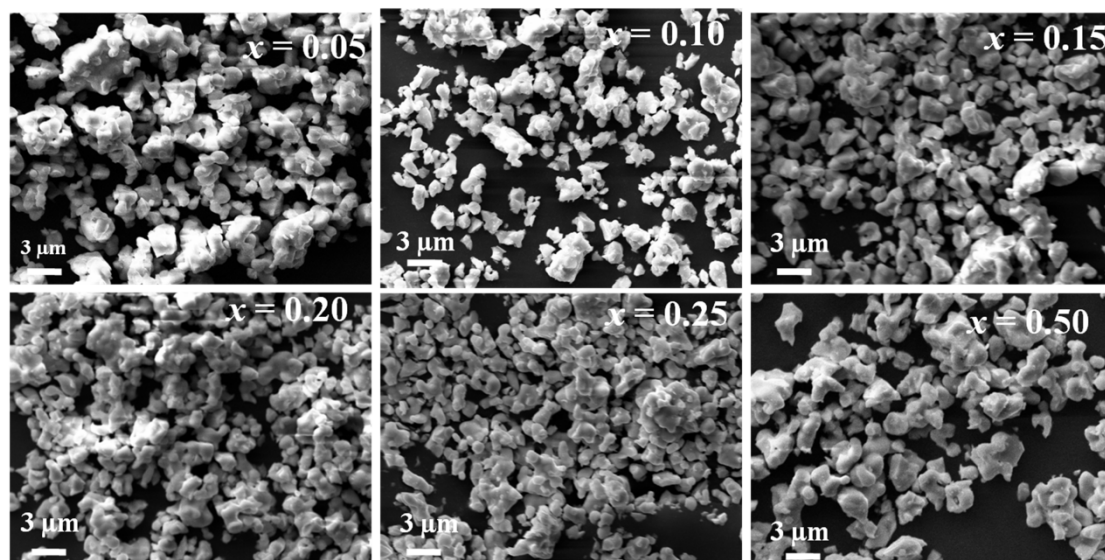


Fig. S5. Typical SEM images of $\text{Y}_2\text{Ce}_{2-x}\text{O}_7:x\text{Eu}^{3+}$ ($x = 0.05, 0.10, 0.15, 0.20, 0.25$ and 0.50) red phosphors. The particles are slightly agglomerated and there is a broad distribution of particle size with an average size of 1-3 μm .